Performance Evaluation of Attitude Estimation Algorithms in the Design of an AHRS for Fixed Wing UAVs

Rogério R. Lima[1] and Leonardo A. B. Tôrres[2]
Programa de Pós-Graduação em Engenharia Elétrica - UFMG
Av. Antônio Carlos, 6627 - Pampulha - Belo Horizonte - MG - Brasil
E-mail: {[1]rlima, [2]torres}@cpdee.ufmg.br

***Abstract*—Three recently published attitude estimation algorithms are compared, and another one is proposed, aiming the performance evaluation when used in an attitude and heading reference system (AHRS), using low cost MEMS sensors, for fixed wing Unmanned Aerial Vehicles. The comparison is based on simulation results associated with typical aerial maneuvers of fixed wing UAVs, characterized by low frequency acceleration signals that are hard to be distinguished from intrinsic sensors biases, as it is usual during coordinated turns. The sensors models are also parameterized from information obtained in the respective datasheets, or obtained from experimental procedures, in order to better represent the imperfections present in practice. Three algorithms are based on the EKF (Extended Kalman Filter) and one is based on nonlinear complementary filtering. The results have revealed that some form of compensation for the effect of low frequency accelerations seems to be crucial to achieve good results.**

***Index Terms*—UAV, AHRS, MEMS sensor, EKF (Extended Kalman Filter), recursive estimation.**

I. Introduction

In the last years, interest in UAVs has grown in both military and civil areas. This seems to be a natural consequence of the availability of processors with high-processing capabilities, high-density batteries, lowpower modems, low-cost MEMS (micro-electro-mechanical systems) sensors and lower cost airframes [1]. Since 2004, projects in this area have been developed at UFMG [2]. In 2010, UFMG has received financial support to build an UAV system which is currently under development by the Research and Development of Autonomous Vehicles (PDVA) group. In this project, an attitude and heading reference system (AHRS) should be built to estimate attitude based on signals from MEMS inertial sensors, magnetometers, GPS receiver, etc.

However, MEMS accelerometers, gyrometers and magnetometers sensors all have intrinsic error sources, e.g. misalignment, cross-coupling sensitivity, bias and noise, that affect them [3][4]. Therefore it is important to take these error sources into account to evaluate, in a more realistic scenario, the performance of attitude estimation algorithms, and this is the main goal of the present work.

In this context, four recursive algorithms are analyzed. Three of them are EKF-based and one is a form of nonlinear complementary filter. The parameters used to set accelerometer, gyrometer and magnetometer models are obtained from sensors datasheets. Typical flight data is generated in a simulation environment where a fixed-wing aircraft model is used to represent a UAV. Three simulated flights are performed, namely: (i) a straight leveled flight mainly used to verify the correctness of the algorithms implementations, specially in relation to gyros biases estimation; (ii) a flight characterized by longitudinal accelerated movement due to pulsed elevator excitation; and (iii) a flight comprised by climb, turn and descent maneuvers found in typical missions of fixed wing UAVs.

The paper is organized as follows. In Section II the sensors mathematical models are presented. In Section III, three recently published attitude estimation algorithms are discussed, and a forth alternative is proposed. In Section IV simulation results for the three types of flight mentioned above are presented, together with their performance evaluation. The main conclusions are registered in Section V.

II. Sensors Modeling

In this section models for accelerometer, gyrometer and magnetometer sensors are developed. Error sources considered in these models are: misalignment, cross-coupling axis, scale factor errors, bias, noise and quantization due to A/D conversion. The proposed error model is based on sensors' specifications from their datasheets. The model is given by

$$\widetilde{m}_s = f_{\mathrm{ADC}}\left(S_s(R_s m_s) + B_s + N_s\right), \tag{1}$$

where the subscript $s = \{a,\ \omega,\ m\}$ defines variables relative to accelerometers, gyrometers and magnetometers, respectively; $\widetilde{m}_s \in \mathbb{R}^{3\times1}$ is the measurement vector; $m_s \in \mathbb{R}^{3\times1}$ is the *ideal* measurement vector; $R_s \in \mathbb{R}^{3\times3}$ is the misalignment matrix; $S_s \in \mathbb{R}^{3\times3}$ is the scale factor and cross-coupling matrix; $B_s \in \mathbb{R}^{3\times1}$ is the bias vector; and $N_s \in \mathbb{R}^{3\times1}$ is the measurement noise vector.

The ideal measurements from accelerometers (m_a) and gyrometers (m_ω) are obtained directly from the simulation model described in Section IV. The ideal magnetometer data (m_m) is obtained from ideal roll (ϕ), pitch (θ) and yaw (ψ) angles and is computed as

$$m_m^b = k_{\mathrm{mag}}\mathbf{R}^{i2b}\begin{bmatrix}\cos(\alpha_{\mathrm{mag}})\\0\\\sin(\alpha_{\mathrm{mag}})\end{bmatrix}, \tag{2}$$

978-0-7695-4906-4/12 $26.00 © 2012 IEEE
DOI 10.1109/SBR-LARS.2012.61

where k_{mag} is the magnitude of geomagnetic field, α_{mag} is the magnetic field declination, and $\mathbf{R}^{i2b}$ is the rotation matrix that relates the vehicle attitude from its reference frame, denoted by b, to the inertial reference frame, denoted by i, such that

$$\mathbf{R}^{i2b} = \begin{bmatrix} C\psi C\theta & S\psi C\theta & -S\theta \\ C\psi S\theta S\phi - S\psi C\phi & S\psi S\theta S\phi + C\psi C\phi & C\theta S\phi \\ C\psi S\theta C\phi + S\psi S\phi & S\psi S\theta C\phi - C\psi S\phi & C\theta C\phi \end{bmatrix}, \quad (3)$$

with S and C representing, respectively, the functions *sin* and *cosine*.

A. Bias

Since bias is the output sensor signal when the sensor input is zero, it can be characterized as stochastic and/or deterministic signal [3]. The deterministic model might be composed by constant or temperature-dependent components, and the stochastic model is considered as the generation of white noise, i.e., with zero mean and constant variance.

The constant bias can be experimentally measured as described in [5] or taken from sensor's datasheet. In general, bias are given in [Ga] for magnetometers, [°/s] for gyrometers and [mg] for accelerometers, with g = $9.81\frac{\text{m}}{\text{s}^2}$ being the gravity acceleration.

The stochastic bias component can be modeled as a pink noise, and might be empirically estimated by registering a long-time observations under constant ambient temperature.

B. Scale Factor and Cross-Coupling Sensitivity

Scale factor is the parameter that represents the conversion from sensor output physical quantity to the physical quantity actually measured by the sensor. Scale factors for analog accelerometers, gyrometers and magnetometers, are generally given by $[\frac{\text{Ga}}{m\text{V}}]$, $[\frac{^{\circ}/\text{s}}{m\text{V}}]$ and $[\frac{m\text{g}}{m\text{V}}]$, respectively. Scale factor errors introduce errors in the sensor's readings. Their effect is modeled by adding perturbations to the main diagonal entries of the matrix

$$S_s = \begin{bmatrix} s_x & s_{xy} & s_{xz} \\ s_{yx} & s_y & s_{yz} \\ s_{zx} & s_{zy} & s_z \end{bmatrix}. \quad (4)$$

The cross-coupling sensitivity, that represents the measurement sensed in an axis when an orthogonal input is applied, is given by nonzero off-diagonal entries of matrix S_s.

C. Inter-axis Misalignment

This parameter models the non-orthogonality of the three sensitive axes. Usually this information is available on the sensors' datasheets and is represented as a single value for all the three misalignment axes. The misalignment matrix is given by

$$R_s = \begin{bmatrix} r_{\hat{x}x} & r_{\hat{x}y} & r_{\hat{x}z} \\ r_{\hat{y}x} & r_{\hat{y}y} & r_{\hat{y}z} \\ r_{\hat{z}x} & r_{\hat{z}y} & r_{\hat{z}z} \end{bmatrix}, \quad (5)$$

where $r_{\hat{j}j}$ is the internal product between the real axis direction $\hat{j}$ and the correspondent ideal axis direction j, with $j = \{x, y, z\}$ representing the subscript for the three orthogonal axes.

D. Noise

Noise is defined as a time-varying signal that is present on the sensor's reading. It is usually modeled as white noise. This information might be readily obtained from datasheets or experimentally estimated from Allan's Variance sensor curve, as described in [6].

The noise variance is given by its power spectral density (PSD) in the units $\left[\frac{m\text{g}}{\sqrt{\text{Hz}}}\right]$ for accelerometers, $\left[\frac{^{\circ}/\text{s}}{\sqrt{\text{Hz}}}\right]$ for gyrometers and $\left[\frac{\text{Ga}}{\sqrt{\text{Hz}}}\right]$ for magnetometers.

E. Quantization

In order to simulate the quantization error introduced in the analog-to-digital conversions, the following function is used

$$f_{\text{ADC}}(V, V_R, b) = \begin{cases} -2^{b-1}, & V \le -V_R \\ \left\lfloor \frac{V}{V_R} 2^{b-1} + \frac{1}{2} \right\rfloor - 2^{b-1}, & \\ 2^{b-1} - 1, & V \ge V_R \end{cases} \quad (6)$$

where b is the number of the bits of the ADC converter, V is the input ADC voltage range and V_R is the ADC reference voltage. It is assumed that the sensors output signals limits are symmetrical around zero.

F. CG Offset for Accelerometers

The positioning of accelerometers out of Center of Gravity - CG contributes to create acceleration components during turns. This affects only accelerometer and not gyros, such that

$$m_a = a_0 + a_{\text{CG}}, \quad (7)$$

where $m_a \in \mathbb{R}^{3\times1}$ is the ideal acceleration measured by accelerometers in $[\frac{\text{m}}{\text{s}^2}]$, $a_0 \in \mathbb{R}^{3\times1}$ is the vehicle linear acceleration and $a_{\text{CG}} = \omega_b \times (\omega_b \times d) + \dot{\omega}_b \times d$ is the acceleration measured due the acceleromenter position located out of vehicle's CG, such that $\omega_b \in \mathbb{R}^{3\times1}$ is the vehicle angular rate in $[\frac{\text{rad}}{\text{s}}]$ and $d \in \mathbb{R}^{3\times1}$ is the displacement of accelerometers from the CG's vehicle in [m].

III. Sensor Fusion Algorithms

In order to choose an attitude estimation algorithm to be implemented in the AHRS, three recursive algorithms recently published in the literature are implemented (algorithms NLCF [7], EKF-7s [8] and mEKF-4s [9]) and a fourth one (Algorithm mEKF-7s) is proposed, which is a modification of the Algorithm mEKF-4s . These algorithms use sensor fusion techniques, based on measurement vector observation built from accelerometers' and magnetometers' readings.

Table I summarizes the main characteristics of each algorithm: gyrometer bias estimation and gravity acceleration correction. The algorithms NLCF and EKF-7s

TABLE I
MAIN CHARACTERISTICS OF THE ALGORITHMS

Algorithm	Bias estimation	Accel. correction
NLCF	x	
EKF-7s	x	
mEKF-4s		x
mEKF-7s	x	x

estimate gyro bias, but do not make any compensation due to vehicle acceleration. On the other hand, Algorithm mEKF-4s compensates the vehicle acceleration, however, it does not estimate the gyro bias. Algorithm mEKF-7s is a modification of Algorithm mEKF-4s to include the estimation of gyros bias.

A. Algorithm NLCF – Nonlinear Complementary Filter

The algorithm proposed in [7] estimates an attitude matrix $\hat{R} \in SO(3)$ and gyrometers' biases $\hat{b}$ using tri-axis inertial sensors and magnetometers.

First, an orientation matrix R is computed utilizing gravity acceleration projections (from accelerometers) and earth magnetic field (from magnetometers) according to

$$R = \left[\frac{h - (g_n^T h) g_n}{\|h - (g_n^T h) g_n\|} \quad \frac{-g_n \times h}{\|h - (g_n^T h) g_n\|} \quad - g_n \right]^T, \qquad (8)$$

with h e g_n being magnetometer's and accelerometer's readings in vehicle's reference frame, respectively.

Following, the orientation matrix $\hat{R}$ is estimated by integrating angular rates (from gyrometers) corrected by estimated bias. In this integration, from the initial condition $\hat{R} = R$ and $\hat{b} = 0$, the estimation of these parameters is propagated in time according to the following differential equations

$$\dot{\hat{R}} = \hat{R}\text{sk}(\hat{\Omega}) \quad \text{and} \quad \dot{\hat{b}} = \Gamma(\hat{R}^T R)^T (X + Y + Z), \qquad (9)$$

in which $\text{sk}(\cdot)$ is a skewed matrix constructor and Γ a nonnegative gain to tune the convergence of gyro bias estimation. $\hat{\Omega}$ is defined as

$$\hat{\Omega} = (\hat{R}^T R)^T (\Omega_m - \hat{b}) - k(X + Y + Z), \qquad (10)$$

with $k > 0$ and $\Omega_m \in \mathbb{R}^{3\times 1}$ are gyrometers' readings. Defining the column vectors from canonical base $\{\epsilon_1, \epsilon_2, \epsilon_3\} \in \mathbb{R}^{3\times 3}$, we have: $\epsilon_1 = [1\ 0\ 0]^T$, $\epsilon_2 = [0\ 1\ 0]^T$ and $\epsilon_3 = [0\ 0\ 1]^T$. Thus, we get $X = (\hat{R}^T \epsilon_1 \times R^T \epsilon_1)$, $Y = (\hat{R}^T \epsilon_2 \times R^T \epsilon_2)$, $Z = (\hat{R}^T \epsilon_3 \times R^T \epsilon_3)$.

The main advantage of this algorithm in attitude estimation is, due to the use of matrix rotation to represent attitude in $SO(3)$, the linearization step present in EKF is eliminated. However, the attitude estimation is only valid if the UAV is not accelerated because, according to the (7), the gravity acceleration used to estimate attitude can be distorted by vehicle accelerations.

B. Algorithm EKF-7s – Standard EKF with 7-states

The attitude and gyro bias estimation algorithm proposed in [8] is a 7-state EKF. The estimation is based on gravity acceleration projection with evolution of attitude represented by quaternions. Process and covariance matrices are considered constants. The proposed EKF has a model with seven states, whose equation of the dynamic system is

$$\begin{aligned} \dot{\mathbf{x}}_B &= \mathbf{f}_B(\mathbf{x}_B, \mathbf{u}_B) + \mathbf{w}_B, \\ \mathbf{y}_B &= \mathbf{h}_B(\mathbf{x}_B) + \mathbf{v}_B, \end{aligned} \qquad (11)$$

with $\mathbf{x}_B = [e_0\ e_1\ e_2\ e_3\ b_p\ b_q\ b_r]^T \in \mathbb{R}^{7\times 1}$ the system state vector in which the first four elements are elements of the attitude quaternion and the last three are gyro's bias; $\mathbf{u}_B = [p\ q\ r]^T \in \mathbb{R}^{3\times 1}$ is the system input composed by gyrometer's reading (angular rates); $\mathbf{y}_B = [a_x\ a_y\ a_z\ \psi_{mag}]^T \in \mathbb{R}^{4\times 1}$ is the measurement vector whose first three elements are accelerometers outputs (gravity projection) and the last one is the heading obtained from magnetometers. $\mathbf{w}_B$ e $\mathbf{v}_B$ are process and measurements noises, respectively; $\mathbf{f}_B(\mathbf{x}_B, \mathbf{u}_B)$ and $\mathbf{h}_B(\mathbf{x}_B)$ are dynamic and output equations, respectively, given by

$$\mathbf{f}_B(\mathbf{x}_B, \mathbf{u}_B) = \begin{bmatrix} \frac{1}{2} \begin{bmatrix} -e_1 & -e_2 & -e_3 \\ e_0 & -e_3 & e_2 \\ e_3 & e_0 & -e_1 \\ -e_2 & e_1 & e_0 \end{bmatrix} \begin{bmatrix} p - b_p \\ q - b_q \\ r - b_r \end{bmatrix} \\ \mathbf{0}^{3\times 1} \end{bmatrix}, \qquad (12)$$

and

$$\mathbf{h}_B(\mathbf{x}_B) = \begin{bmatrix} 2g(e_1 e_3 - e_0 e_2) \\ 2g(e_2 e_3 + e_0 e_1) \\ g(e_0^2 - e_1^2 - e_2^2 + e_3^2) \\ \tan^{-1}\left(\frac{2(e_1 e_2 + e_0 e_3)}{e_0^2 + e_1^2 - e_2^2 - e_3^2}\right) \end{bmatrix}. \qquad (13)$$

C. Algorithm mEKF-4s – Modified EKF with 4-states

The Algorithm mEKF-4s , described in [9], is an EKF-based algorithm similar to the Algorithm EKF-7s , however its state vector has four elements because the gyros' biases are not estimated. So, dynamic system is given by

$$\begin{aligned} \dot{\mathbf{x}}_C &= \mathbf{f}_C(\mathbf{x}_C, \mathbf{u}_C) + \mathbf{w}_C, \\ \mathbf{y}_C &= \mathbf{h}_C(\mathbf{x}_C) + \mathbf{v}_C. \end{aligned} \qquad (14)$$

with

$$\mathbf{f}_C(\mathbf{x}_C, \mathbf{u}_C) = \begin{bmatrix} \frac{1}{2} \begin{bmatrix} -e_1 & -e_2 & -e_3 \\ e_0 & -e_3 & e_2 \\ e_3 & e_0 & -e_1 \\ -e_2 & e_1 & e_0 \end{bmatrix} \begin{bmatrix} p \\ q \\ r \end{bmatrix} \end{bmatrix}. \qquad (15)$$

An important characteristic of this algorithm is the compensation that is made in accelerometers' readings. The gravity acceleration, that is distorted when the UAV executes dynamic maneuvers, is calculated by compensating the accelerometers readings (a_x, a_y, a_z) from linear velocities (U, V, W) and accelerations $(\dot{U}, \dot{V}, \dot{W})$ and angular rates (p, q, r), as can be seen below

$$\begin{aligned} g_x &= a_x - [\dot{U} + (Wq - Vr)], \\ g_y &= a_y - [\dot{V} + (Ur - Wp)], \\ g_z &= a_z - [\dot{W} + (Vp - Uq)]. \end{aligned} \qquad (16)$$

This compensation theoretically improves the filter performance during accelerated maneuvers. Velocities U, V and W are obtained from ground speed information (V_N,

V_E and V_D are north, east and down velocities) from GPS receiver through the rotation matrix $\mathbf{R}^{i2b}$:

$$\begin{bmatrix} U \\ V \\ W \end{bmatrix} = \mathbf{R}^{i2b} \begin{bmatrix} V_N \\ V_E \\ V_D \end{bmatrix}. \quad (17)$$

Velocities' rate $\dot{U}$, $\dot{V}$ and $\dot{W}$ are computed from $\dot{V}_N$, $\dot{V}_E$ and $\dot{V}_D$ by (17) and are calculated using linear approximations:

$$\dot{V}_N = \frac{V_N^k - V_N^{k-1}}{T_{GPS}}, \quad \dot{V}_E = \frac{V_E^k - V_E^{k-1}}{T_{GPS}}, \quad \dot{V}_D = \frac{V_D^k - V_D^{k-1}}{T_{GPS}}, \quad (18)$$

where T_{GPS} is the GPS update time. Since the velocities' rates are calculated from (18), their uncertainties are amplified by the factor $\sqrt{2}$, considering T_{GPS} constant. In this way, in order to decrease those uncertainties, velocity estimation algorithms that use time-differential carrier-phase as in [10], which provides better results, should be considered.

The output equation $\mathbf{h}_C(\mathbf{x_C})$ gives the Euler angles directly and includes the unit norm constraint for quaternions as follows

$$\mathbf{h}_C(\mathbf{x}_C) = \begin{bmatrix} \tan^{-1}\left(\frac{2(e_0e_1+e_2e_3)}{e_0^2-e_1^2-e_2^2+e_3^2}\right) \\ \sin^{-1}(2(e_1e_3 - e_0e_2)) \\ \tan^{-1}\left(\frac{2(e_1e_2+e_0e_3)}{e_0^2+e_1^2-e_2^2-e_3^2}\right) \\ e_0^2 + e_1^2 + e_2^2 + e_3^2 \end{bmatrix}. \quad (19)$$

In the implementation of Algorithm mEKF-4s, the unit norm constraint in (19) was not considered because the quaternion normalization is done in every algorithm's iteration.

The process and measurement covariance matrices are state-dependent and were formulated considering only first order terms of the Taylor series expansion.

D. Algorithm mEKF-7s – Modified EKF with 7-states

The Algorithm mEKF-7s is a modified version of Algorithm mEKF-4s with the state vector augmented from four to seven states to include gyro's bias estimation. Thus, the equation of the dynamic system is given by

$$\mathbf{f}_D(\mathbf{x}_D, \mathbf{u}_D) = \begin{bmatrix} \frac{1}{2}\begin{bmatrix} -e_1 & -e_2 & -e_3 \\ e_0 & -e_3 & e_2 \\ e_3 & e_0 & -e_1 \\ -e_2 & e_1 & e_0 \end{bmatrix} \begin{bmatrix} p - b_p \\ q - b_q \\ r - b_r \end{bmatrix} \\ \mathbf{0}^{3\times 1} \end{bmatrix}, \quad (20)$$

where $\mathbf{x}_D = [e_0 \ e_1 \ e_2 \ e_3 \ b_p \ b_q \ b_r]^T \in \mathbb{R}^{7\times 1}$ is the augmented state vector and $\mathbf{u}_D = [p \ q \ r]^T \in \mathbb{R}^{3\times 1}$ is the input vector. The output equation is defined as $\mathbf{h}_D(\mathbf{x}_D) = \mathbf{h}_C(\mathbf{x}_D)$.

IV. Simulations

In order to evaluate the performance of algorithms NLCF , EKF-7s , mEKF-4s and mEKF-7s , simulated data were produced using the simulation software MATLAB©/Simulink to generate flight data and to implement the algorithms.

The flight data generation is based on a flight simulation in which a fixed-wing aircraft is modeled as a rigid body with 6DOF (degrees-of-freedom) as described in [11]. The model's mass, geometric and aerodynamic data were taken from [12].

The following ideal data generated are: roll, pitch and heading angle (ϕ,θ,ψ); linear accelerations (a_x, a_y, a_z); angular rates (p, q, r) and linear velocities (U, V, W), all of them generated at 50 Hz. It is considered that linear velocities are measured from a 5 Hz GPS, so to make simulation more realistic, linear velocities V_N, V_E and V_D are decimated to get appropriate sample rate (5 Hz). Uncertainties for GPS velocities are modeled as white noise with variance $1.6 \times 10^{-3} \frac{\mathrm{m}^2}{\mathrm{s}^2}$, which values were obtained from [10] for a stand-alone GPS. Velocities rates variance are $1.6\sqrt{2} \times 10^{-3} \frac{\mathrm{m}^2}{\mathrm{s}^4}$.

A. Parameters of the Error Models

The sensors chosen were the accelerometer ADXL345 [13], gyrometer ITG-3200 [14] and the magnetometer HMC5883L [15], whose main characteristics are listed in the table below.

TABLE II
Typical values for the sensors

Parameters	Accel	Gyro	Mag
Bias	40 mg	3 °/s	n.a.
Scale factor	10%	6%	5%
Cross coupling	1%	2%	0.2%
Misalignment	0.1°	0.1°	n.a.
Noise	$\frac{2mg}{\sqrt{\mathrm{Hz}}}$	$\frac{0.03°/\mathrm{s}}{\sqrt{\mathrm{Hz}}}$	2 mGa
ADC resol.	10-bits	16-bits	12-bits
Quantization	0.0039g	0.0092 °/s	0.0012 Ga

All available information in datasheets required to fill the accelerometer, gyrometer and magnetometer models in (1) are:

$$S_a = \begin{bmatrix} 0.98 & 0.01 & 0.01 \\ 0.01 & 1.01 & 0.01 \\ 0.01 & 0.01 & 0.99 \end{bmatrix}, \ B_a = \begin{bmatrix} 40 \\ 40 \\ 40 \end{bmatrix} mg, \ N_a = \begin{bmatrix} \sigma_{a_x} \\ \sigma_{a_y} \\ \sigma_{a_z} \end{bmatrix},$$

$$S_\omega = \begin{bmatrix} 1.01 & 0.02 & 0.02 \\ 0.02 & 0.99 & 0.02 \\ 0.02 & 0.02 & 0.98 \end{bmatrix}, \ B_\omega = \begin{bmatrix} 2 \\ 3 \\ 4 \end{bmatrix} °/\mathrm{s}, \ N_\omega = \begin{bmatrix} \sigma_p \\ \sigma_q \\ \sigma_r \end{bmatrix},$$

$$S_m = \begin{bmatrix} 1.00 & 0.00 & 0.00 \\ 0.00 & 1.00 & 0.00 \\ 0.00 & 0.00 & 1.00 \end{bmatrix}, \ B_m = \begin{bmatrix} 0 \\ 0 \\ 0 \end{bmatrix} \mathrm{Ga}, \ N_m = \begin{bmatrix} \sigma_{m_x} \\ \sigma_{m_y} \\ \sigma_{m_z} \end{bmatrix},$$

where $\sigma^2_{a_{\{x,y,z\}}}$, $\sigma^2_{\{p,q,r\}}$ and $\sigma^2_{m_{\{x,y,z\}}}$ are, respectively, accelerometers, gyrometers and magnetometers variances which values are listed in Table III. Since misalignment errors are negligible if compared to the other error sources, is considered that the three axes sensors are perfectly orthogonal, i.e. $R_a = R_\omega = R_m = I_3$

B. Algorithm's parameters

In Algorithm NLCF , after a trial and error process, it was chosen $\Gamma = 1$ that influences the convergence of the

TABLE III
SENSORS' VARIANCES USED IN THE SIMULATIONS.

Sensor	Variance symbol	Value	Unit
Accelerometer	$\sigma^2_{a_x}, \sigma^2_{a_y}, \sigma^2_{a_z}$	4×10^{-6}	$[\frac{m^2}{s^4}]$
Gyrometer	$\sigma^2_p, \sigma^2_q, \sigma^2_r$	8.1×10^{-5}	$[\frac{rad^2}{s}]$
Magnetometer	$\sigma^2_{m_x}, \sigma^2_{m_y}, \sigma^2_{m_z}$	4×10^{-6}	$[Ga^2]$
GPS	$\sigma^2_U, \sigma^2_V, \sigma^2_W$	1.6×10^{-3}	$[\frac{m^2}{s^2}]$
GPS	$\sigma^2_U, \sigma^2_V, \sigma^2_W$	3.2×10^{-3}	$[\frac{m^2}{s^4}]$

gyro bias estimation and $k = 2.5$ the gain of orientation matrix estimation.

In the Algorithm EKF-7s , the process and measurement covariance matrices were built as $Q_B = \text{diag}(\sigma^2_{e_0}, \sigma^2_{e_1}, \sigma^2_{e_2}, \sigma^2_{e_3}, \sigma^2_{b_p}, \sigma^2_{b_q}, \sigma^2_{b_r})$ where $\sigma^2_{e_0} = \sigma^2_{e_1} = \sigma^2_{e_2} = \sigma^2_{e_3} = 1 \times 10^{-6}$ are quaternion variances and $\sigma^2_{b_p} = \sigma^2_{b_q} = \sigma^2_{b_r} = 1 \times 10^{-6}$ $[\frac{rad^2}{s^2}]$ are gyro biases variances, and $R_B = \text{diag}(\sigma^2_{a_x}, \sigma^2_{a_y}, \sigma^2_{a_z}, \sigma^2_{\phi_{mag}})$ where $\sigma^2_{\phi_{mag}} = 1 \times 10^{-4}$ [rad^2] is the variance of yaw angle.

For Algorithm mEKF-4s , the process covariance matrix was chosen as $Q_C = \text{diag}(\sigma^2_p, \sigma^2_q, \sigma^2_r)$ where $\sigma^2_p, \sigma^2_q, \sigma^2_r$ are gyro variances showed in Table III. The measurement covariance matrix R_C, which is built from information about sensor noises as proposed in [9], have variances listed in the Table III. The variance of quaternion constraint is $\sigma^2_C = 1 \times 10^{-10}$.

In the Algorithm mEKF-7s , the process covariance matrix was augmented to include gyro bias variances and is assigned as $Q_D = \text{diag}(\sigma^2_p, \sigma^2_q, \sigma^2_r, \sigma^2_{b_p}, \sigma^2_{b_q}, \sigma^2_{b_r})$ with gyro bias variance $\sigma^2_{b_p} = \sigma^2_{b_q} = \sigma^2_{b_r} = 1 \times 10^{-6}$ $[\frac{rad^2}{s^2}]$. The measurement covariance matrix R_D is computed as R_C using the same sensors noise information for the R_C matrix.

C. Performance Evaluation

To evaluate the algorithms under analysis, three different flights were simulated. The Flight 1 is a straight leveled flight, just to check convergence of biases estimation. The Flight 2 is a leveled flight corresponding to the application of a doublet in the elevator as an input command to the aircraft model leading to longitudinal acceleration. The Flight 3 is composed by maneuvers such as climb, turns and descent, in a manner to evaluate the estimation of the three angles of attitude in a typical mission.

Fig. 1 shows the estimated attitude for the Flight 1. It can be seen that Algorithm NLCF estimates attitude with errors lower than 1°, while EKF-7s and mEKF-7s show good estimation in a non-accelerated flight, see estimation errors in the Table IV for Flight 1 results. Gyro bias is estimated and used to correct the gyros' readings as can be seen in Fig. 2. However, Algorithm mEKF-4s presents larger errors probably because there is no gyro bias estimation for proper correction.

Fig. 3 shows the attitude estimation for the Flight 2 in which is applied a doublet in the elevator ($t = 10$s). As can be seen in Table IV, Algorithm mEKF-7s has presented better results than others algorithms. It can

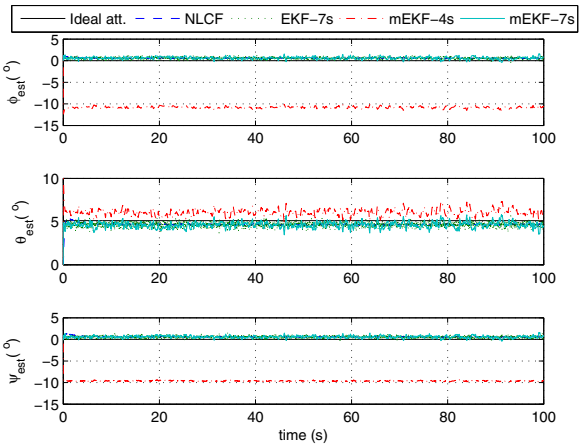

Fig. 1. Estimated attitude for Flight 1.

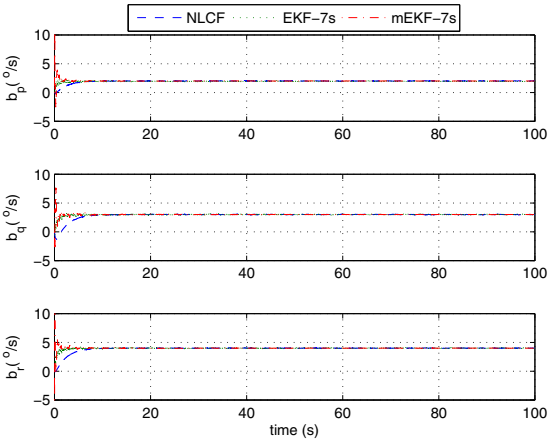

Fig. 2. Estimated bias for Flight 1.

be explained possibly because when aircraft is diving or climbing, gravity accelerations measured by accelerometers are distorted due to vehicle's acceleration, and than errors in the estimated attitude are too distorted if none correction is done.

Fig. 4 exhibits results for the Flight 3, composed by maneuvers like climb ($t = 10$s), turns to the right ($t = 25$s) and to the left ($t = 30$s) and descent. Here, Algorithm mEKF-7s shows better results if compared to the others algorithms and can track ideal attitude with lower errors, as can be seen in Table IV.

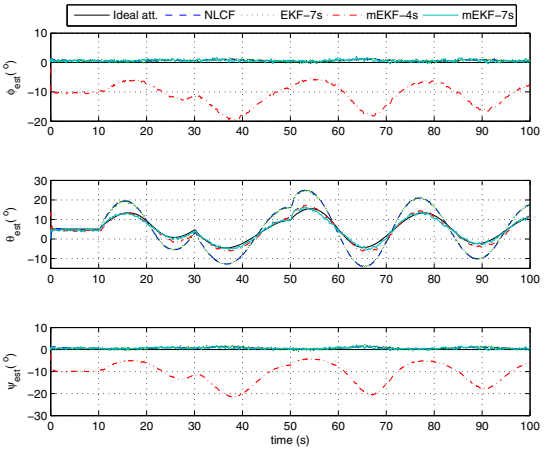

Fig. 3. Estimated attitude for Flight 2.

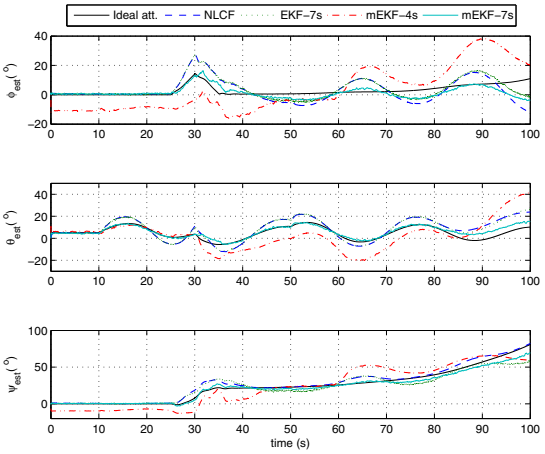

Fig. 4. Estimated attitude for Flight 3.

TABLE IV
MAXIMUM ABSOLUTE ERROR (IN DEGREES) IN THE ATTITUDE ESTIMATION FOR FLIGHTS 1, 2 AND 3.

		Algorithms			
	angle	NLCF	EKF-7s	mEKF-4s	mEKF-7s
Flight 1	ϕ	0.77	1.54	11.12	1.62
	θ	0.64	1.45	1.94	1.65
	ψ	0.81	1.67	10.27	1.61
Flight 2	ϕ	1.25	1.87	19.45	2.05
	θ	10.41	10.92	3.48	2.70
	ψ	1.40	2.41	21.62	2.18
Flight 3	ϕ	15.19	13.67	22.76	10.84
	θ	14.56	15.00	19.23	6.68
	ψ	12.55	18.84	32.67	10.94

V. Conclusion

This work has dealt with errors sensor modeling of tri-axis accelerometers, gyrometers and magnetometers to evaluate the performance of attitude estimation algorithms. Error sources like misalignment, cross-coupling, scale factor errors, quantization errors, bias and noise, whose information were obtained from respective sensors' datasheet, were considered. Four recursive algorithms designed to estimate attitude were evaluated, in which three are EKF-based and one is a nonlinear complementary filter. The best results were achieved by the proposed Algorithm mEKF-7s , by combining vehicle acceleration corrections and gyro bias estimation in a single algorithm. The results showed that in dynamic maneuvers, error in estimated attitude is larger in those algorithms which do not make any compensation in gravity acceleration. Therefore, it is important to highlight that vehicle acceleration seems to be the major source of estimation errors, since it is common practice to use gravity projection to infer attitude.

Acknowledgment

This work has been supported by the Brazilian agencies CAPES, CNPq, and FINEP. The authors also thank the graduate program PPGEE/UFMG for the financial support.

References

[1] H. Chao, Y. Cao, and Y. Chen, "Autopilots for Small Fixed-Wing Unmanned Air Vehicles: A Survey," *2007 International Conference on Mechatronics and Automation*, pp. 3144–3149, Aug. 2007.

[2] P. Iscold, G. a. S. Pereira, and L. a. B. Torres, "Development of a Hand-Launched Small UAV for Ground Reconnaissance," *IEEE Transactions on Aerospace and Electronic Systems*, vol. 46, no. 1, pp. 335–348, Jan. 2010.

[3] G. Xin, Y. Dong, and G. Zhen-hai, "Study on Errors Compensation of a Vehicular," *Science And Technology*, pp. 205–210, 2005.

[4] H. Jiang, H. Jia, Q. Wei, and X. Zhang, "Distribution of Gyroscope Accuracy Parameters for E-O Stabilization Platform," *Sciences-New York*, 2011.

[5] A. Young and M. Ling, "IMUSim: A Simulation Environment for Inertial Sensing Algorithm Design and Evaluation," *Environment*, 2011.

[6] L. Iozan, C. Rusu, J. Collin, and J. Takala, "A Study of the External Factors that Affect the Measurement Data of a MEMS Gyroscope Sensor – Towards an Inertial Navigation System," in *Electronics and Telecommunications (ISETC), 2010 9th International Symposium on.* IEEE, 2010, pp. 81–84.

[7] J. M. Pflimlin, T. Hamel, and P. Souères, "Nonlinear attitude and gyroscope's bias estimation for a vtol uav," *Intern. J. Syst. Sci.*, vol. 38, no. 3, pp. 197–210, Jan. 2007.

[8] J. Jang and D. Liccardo, "Automation of Small UAVs using a Low Cost Mems Sensor and Embedded Computing Platform," *2006 ieee/aiaa 25TH Digital Avionics Systems Conference*, pp. 1–9, Oct. 2006.

[9] D.-M. Ma, J.-K. Shiau, I.-C. Wang, and Y.-H. Lin, "Attitude Determination Using a MEMS-Based Flight Information Measurement Unit." *Sensors (Basel, Switzerland)*, vol. 12, no. 1, pp. 1–23, Jan. 2012.

[10] J. Zhou, S. Knedlik, and O. Loffeld, "INS/GPS for High-Dynamic UAV-Based Applications," *International Journal of Navigation and Observation*, vol. 2012, pp. 1–11, 2012.

[11] B. L. Stevens and F. L. Lewis, *Aircraft Control and Simulation.* Wiley-Interscience, Oct. 2003.

[12] FixedWingModel, *Aircraft data*, 2012 (accessed April 14, 2012). [Online]. Available: http://www.flightgear.org

[13] AnalogDevices, *3-Axis Digital Accelerometer ADXL345*, 2012 (accessed May 20, 2012). [Online]. Available: http://www.analog.com

[14] InvenSense, *3-Axis MEMS Digital Gyrometer ITG-3200*, 2012 (accessed May 20, 2012). [Online]. Available: http://www.invensense.com

[15] Honeywell, *3-Axis Digital Compass IC HMC5883L*, 2012 (accessed May 20, 2012). [Online]. Available: http://www.honeywell.com